The Thermoresponsive Shape Memory Characteristics of Polyurethane Foam

Seung Eun Chung,[1] Chung Hee Park[2]

[1]*Intelligent Textile System Research Center, Seoul, Korea*
[2]*Department of Clothing and Textiles, Seoul National University, Seoul, Korea*

Received 18 October 2009; accepted 25 December 2009
DOI 10.1002/app.32003
Published online 13 April 2010 in Wiley InterScience (www.interscience.wiley.com).

ABSTRACT: The purpose of this study is to develop a protective and thermally intelligent filler by optimizing the preparing conditions and the thermoresponsive property of PU foam. The specimens were polyurethane synthesized by a one step process with 4,4′-diphenylmethane diisocyanate, polycaprolactone and 1,4-butanediol. After dissolving the polyurethane in tetrahydrofuran, the polyurethane foam was manufactured by the salt leaching method. The appearance, compressive property, and thermal property of the manufactured foam as well as the shape memory effects were evaluated. In addition, air and water vapor permeabilities and the thermal insulation property were measured to examine the basic properties of the foam. The cell sizes of the completed foam were distributed in the range of 400–1,000 μm. The compressive stress of the foam was low in the initial compressive strain but increased dramatically above a compressive strain of 70%. However, the foam showed a very low capacity for compressive stress compared with an electrospun web or a film manufactured by using the identical shape memory polyurethane. The transition temperature of the foam was 30°C. The shape recovery and shape retention were 98% or higher. The foam, with a porous structure, was found to be generally good in both air and water vapor permeability. In the case of the foam that maintained its compressed shape below the transition temperature, these permeabilities of the foam decreased slightly, but not significantly. Because of the porous structure of the foam, the shape memory effect did not noticeably influence the permeability change with a change in temperature. © 2010 Wiley Periodicals, Inc. J Appl Polym Sci 117: 2265–2271, 2010

Key words: polyurethanes; foams; fillers; nanotechnology; high performance polymers

INTRODUCTION

Shape memory polymers (SMPs) are smart polymers that, as a result of an external stimulus, can change from a temporary deformed shape back to its original shape.[1–5] SMPs have drawn an increasing attention because of their scientific and technological significance.[6–8] They offer a much higher degree of deformation and a wider scope in their varying mechanical properties compared with shape memory alloys or ceramics, in addition to their inherent advantages of being cheap, light weight, and easily processable. Polymers offer many extra advantages because they may be biocompatible, nontoxic, and can be made biodegradable.[9] Thus, SMPs can be manufactured in various forms and have been widely made as film shaped thin and poreless membranes.[10–14] However, the film-shaped SMPs were limited in their shape memory effect performance and needed to be improved in such things as the permeability change with temperature because of their poreless structure. Therefore, in our previous research, electrospun web was manufactured and its performance was evaluated to investigate the obvious shape memory effects. As a result, the electrospun web showed excellent water vapor and air permeabilities because its structural characteristics incorporate countless nano-sized pores. Because of this, the electrospun web maintained its expanded state below the transition temperature, as shown by the improved permeabilities.

SMPs can also be manufactured in a type of foam and several studies on SMP foams were reported.[15–22] SMP foams have low density, high compressibility, and an excellent shape memory.[15–17] Studies on SMP foams have been performed in the aerospace and biomedical fields, and other fields using industrial technology[18–21] where the low density of the foam offsets the relatively lower mechanical properties when compared with solid SMPs. However, there have not been sufficient relevant researches. Moreover, the shape memory polyurethane (SMPU) foam has an energy absorption property and a heat insulating property.[15–17] Lightweight, with a significant shape recovery, SMP foams can be used for quick molding

Correspondence to: C. H. Park (junghee@snu.ac.kr).
Contract grant sponsor: The Korea Science and Engineering Foundation (KOSEF), The Korea government (MEST); contract grant number: R11-2005-065.

© 2010 Wiley Periodicals, Inc.

into a particular shape.[22] As SMPU foams have these superior qualities, applications using the SMPU foams are expected in many fields.[18] When the SMPU foam is manufactured by taking advantages of these capabilities, it is expected to be used as an intelligent material that is capable of heat insulation under high temperature conditions and shape memorization. Polyurethane foam is manufactured generally by the process of chemical foaming. However, the salt leaching method is widely used to manufacture foam for biomaterials. This method makes the manufacturing process simple and helps to readily control the pore size and the porosity of a structure by adjusting the size and the amount of the salt particles.[23,24]

Therefore, for this research, SMPU foam was manufactured by the salt leaching method to investigate its performance as a smart material. We examined the physical properties, the shape memory effect, the permeability, and the thermal insulation after making foam that can change its thickness according to temperature. In addition, the permeability and the thermal insulation changes caused by the shape memory behavior were evaluated.

EXPERIMENTAL

Materials

Poly(ε-caprolactone) diol(PCL diol, M_n = 4,000 g/mol), 4,4′-diphenylmethane diisocyanate (MDI), and 1,4-butanediol (BD) were provided and synthesized by the Hosung Chemex. Co. The molar ratio for this polyurethane(M_w = 270,000g/mol) synthesis was 6 : 1 : 5 for MDI : PCL : BD.

Preparation of the specimen

For the manufacturing of the foam, the polyurethane was dissolved in tetrahydrofuran (THF) to make solutions with concentrations ranging from 7 to 9 wt % and NaCl was prepared. After blending the polyurethane solution with the NaCl evenly, the mixed solution was poured into Teflon frame to form a shape. The solution was dried in 20°C ± 3 and 40 ± 5% RH for 2∼3 days until the THF was volatilized completely. The dried specimen was immersed in water to dissolve the NaCl completely before the specimen was dried at room temperature. The specimen was manufactured with a thickness of 20 mm in consideration of the case where the specimen would be used as a filler for clothing.

To make the reference film, polyurethane chips were melted down and compressed using hot plates. To manufacture the nanowebs, a polyurethane solution of 4 wt % was electrospinned at 20 ± 3°C and 50 ± 10% RH, adjusting the voltage to 6.5 kV, with a feed rate of 1.0 ml/h, and a spinning distance of 15 cm. A 1 : 1 mixture of N, N-dimethylformamide (DMF) and tetrahydrofuran (THF) was used as a solvent.

Compressive property

To measure the compressive property, the specimens were prepared with a size of 20 mm (length) × 20 mm (width) × 20 mm (thickness). Steel plates were fixed on the jaws of the Universal Testing Machine (UTM) used for the compression test before placing the specimen between the steel plates. The compressive stress–strain curve was measured until the specimen was compressed to a maximum. The cross head speed was set at a rate of 10 mm/min.

Thermal property

A differential scanning calorimeter (DSC Q-1000, TA Instrument, UK) was employed to detect the transition temperature from −20°C up to 250°C at a heating rate of 10°C/min.

Thermomechanical property

To evaluate the shape memory effect, the foams were prepared with a size of 20 mm (length) × 20 mm (width) × 20 mm (thickness). They were compressed 80% at T_{trans} + 20°C and cooled off to T_{trans} − 20°C. The load was then removed and the cooling state was maintained for 10 min. The specimens were again heated up to T_{trans} + 20°C and maintained for 10 min. Shape retention and shape recovery were acquired based on the following equations:

$$\text{Shape retention}(\%) = \varepsilon f/\varepsilon m \times 100 \quad (1)$$

$$\text{Shape recovery}(\%) = \{(\varepsilon m - \varepsilon r)/\varepsilon m\} \times 100 \quad (2)$$

εm = The strain at an 80% compression

εf = The strain at T_{trans} − 20°C

εr = The recovery compression rate at T_{trans} + 20°C

Based on the results of the compression test, in the free recovery test the specimen was compressed by 80% at T_{trans} + 20°C before being cooled off at T_{trans} − 20°C for 10 min. The fixed specimens were put into chambers set at 20, 30, 40, and 50°C. During recovery, the exact temperature, time, and height (in % with respect to the original specimen height) were recorded.

Appearance

The specimens were observed with a Field Emission Scanning Electron Microscope (FE-SEM, SUPRA

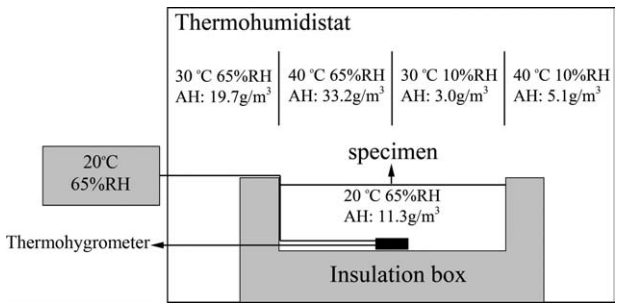

Figure 1 The thermal insulation measuring system.

55VP, Carl Zeiss, Germany) to check out the cell size and uniformity.

Air permeability and water vapor transmission rate

The air permeability was measured with an ASTM D 737 and the water vapor transmission rate was measured with a testing method using calcium chloride per ASTM E 96.

Thermal insulation property

To evaluate the thermal insulation property under high temperature conditions, an insulation box with an interior space of 100 mm × 100 mm × 30 mm was constructed. After controlling the inner environment of the test chamber with the heat-insulation box at 20°C and 65% RH, the upper area of the heat insulation box was completely sealed. The chamber environment was adjusted at the rate of 3.3°C/min to the temperatures of 30°C and 40°C and the humidity was controlled from 65% RH to 10% RH. The thermal insulation measuring system of the specimens is shown in Figure 1.

RESULTS AND DISCUSSION

Optimal conditions for the foam formation and appearance

For this research, the SMPU foams were manufactured by the salt leaching method. After blending polyurethane solution with NaCl evenly and pouring the mixed solution into a Teflon frame, the mixed solution was dried until the solvent was volatilized completely. The optimal foam was formed when THF was used as a solvent to produce a polyurethane solution of 9 wt % before blending the solution and NaCl at the ratio of 10 : 7 ~ 8 (v : v). The density of the manufactured foam was about 0.11 g/cm^3. When the solution concentration was too low, or the NaCl content was too high, the shape was not preserved after the mixed solution was dried. On the contrary, when the NaCl content was too low, sufficient space was not formed in the inside of the foam.

The cross-sectional image of the foam is shown in Figure 2. The cell sizes of the foam were in the range of 426~1046 μm while the average cell size of the foam was 640 μm. The cells are created as the space that the NaCl took up dissolved. Therefore, the cell size tends to be proportional to the size of the NaCl particle. As shown in Figure 2(b), the sizes of the NaCl particles were in the range of 343~463 μm with an average diameter of 394 μm. It was shown that the cell size of the foam was about 1.6 times bigger than the size of the NaCl particles. These results may be attributable to the possibility that the NaCl particles were aggregated in the process of blending the NaCl with the polyurethane solution or to the possibility of the solvent being volatilized. In the 9 wt % polyurethane solution, the solvent probably takes up more volume than the solute. As a result, it can be inferred that the cell size increased as the solvent volatilized and the space occupied by the solvent turned into a cell.

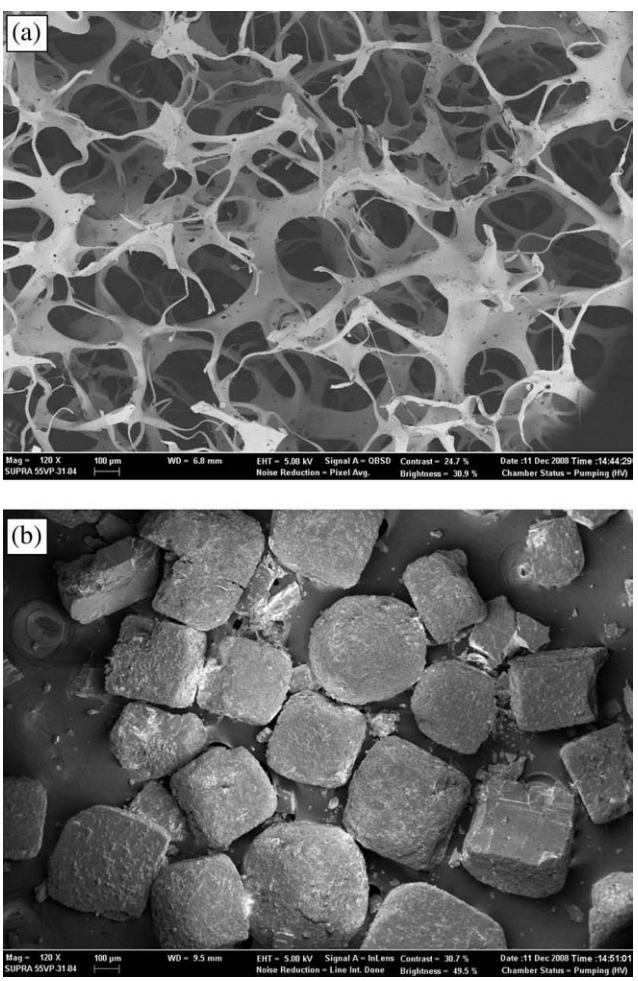

Figure 2 (a) The field-emission scanning electron microscopic pictures of the polyurethane foam. (b) The field-emission scanning electron microscopic pictures of the salt particles.

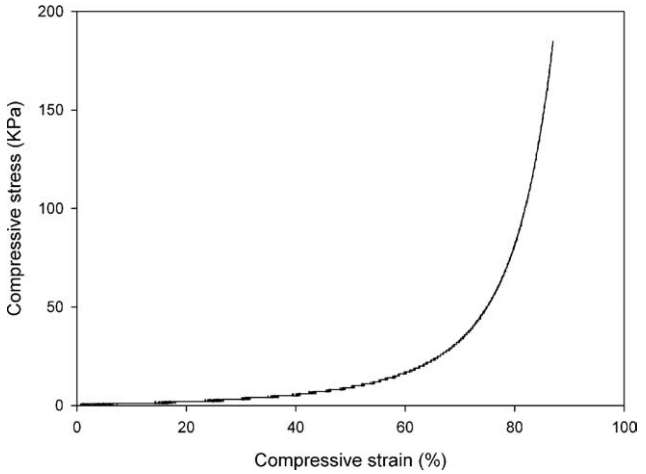

Figure 3 The compressive stress–strain curve of the foam measured at a compressive strain rate of 10 mm/min.

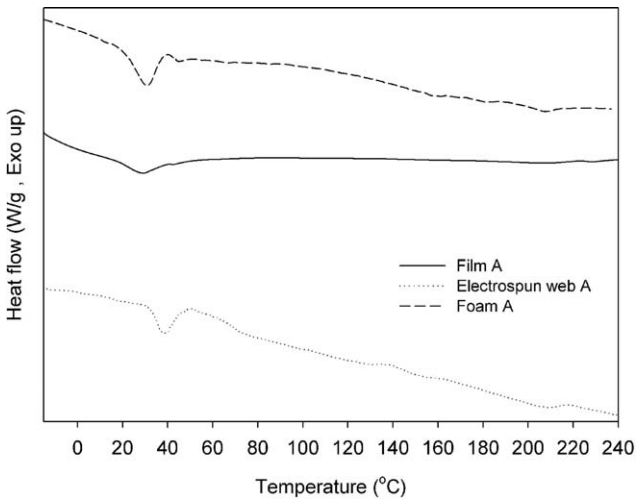

Figure 4 The DSC diagram of the film, the electrospun web and the foam measured at a heating rate of 10°C/min.

Compressive property

Figure 3 shows the compressive property of the SMPU foam. The compressive stress was very low in the beginning, however, the compressive stress was found to increase dramatically above a compressive strain of 70%. The foam was compressed up to 87%, at that point the stress value was 185 KPa, which was very low compared with the SMPU electrospun web or the film in our previous research. As a result, it can be surmised that the foam is suitable for shape transforming or recovery, because the foam requires a very low energy to change or maintain shape.

Thermal property

Table I and Figure 4 shows the results of the DSC analysis of the SMPU foam. The foam showed an endothermic peak by soft segment melting at 30.7°C. In our previous research, the film and the electrospun web manufactured by the identical SMPU material showed endothermic peaks by soft segment melting at 29.1 and 38.2°C, respectively. Compared with the film and the electrospun web, the foam showed a transition temperature similar to that of the film but a higher value of fusion heat. This means that, although the foam is not expected to have a fiber orientation effect in the spinning process as in the case of the electrospun web, it is more suitable for soft segment crystal formation than the film is as it is dried at a room temperature for a long time. This explains the reason why the foam showed a high fusion heat.

TABLE I
The Melting Temperatures and the Heat of Fusion for Film, Electrospun Web, and Foam

Sample	Soft segment melt temperature (°C)	Heat of fusion (J/g)
Film	29.1	7.1
Electrospun web	38.2	10.9
Foam	30.7	10.5

Shape memory effect

As shown in Figure 5, the foam showed a 98% and a 99% of shape retention and shape recovery, respectively, which is an excellent capability for shape memory. The foam has a soft segment crystal structure that is highly developed and so takes up a great deal of space inside the foam due to its structural properties. Therefore, a slight force can cause shape transformation. Consequently, in the case of the foam as compared with the film or the electrospun

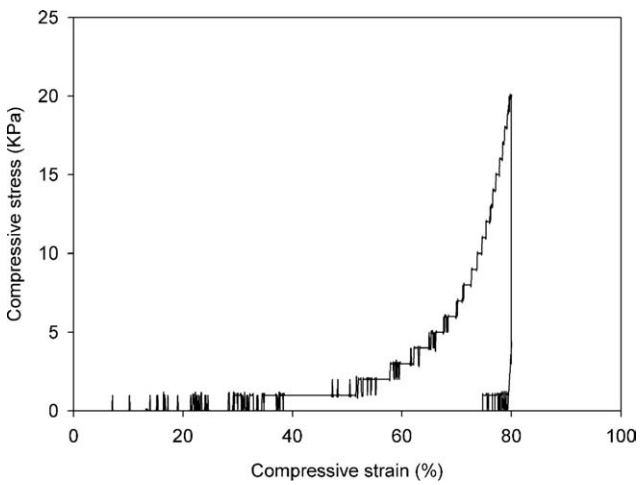

Figure 5 The compressive stress–strain curves for the shape memory behavior of the foam at a compressive strain rate of 5 mm/min.

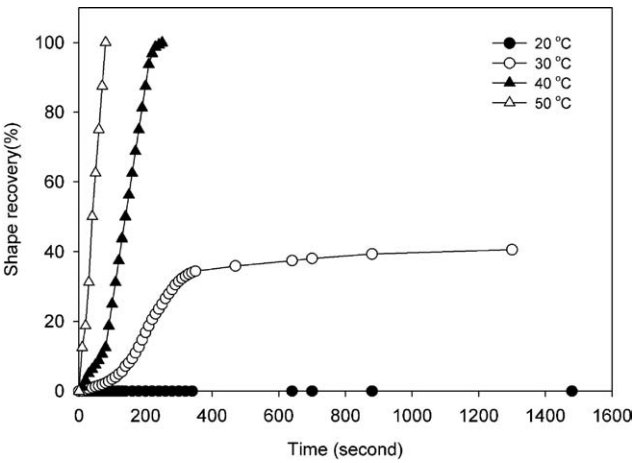

Figure 6 The shape recovery behavior for the foam measured at 20, 30, 40, and 50°C.

web, the transformation of the inside structure of the specimen due to shape transformation can be kept at a minimum. Because of this, the shape memory effect seemed to be improved.

Figure 6 shows the results of the free recovery test according to the temperatures of the SMPU foam. There was no change in the foam shape at 20°C, while there was an observed partial recovery of the foam shape, less than 50%, at 30°C. At 40°C or higher, it took more time for the shape recovery than at 50°C, but the foam recovered to its original shape almost completely. As shown in Figure 7, around 80 s was required for shape recovery at 50°C, which is a relatively quick shape recovery.

Air permeability and water vapor transmission rate

As shown in Figure 8, the foam showed an air permeability similar to the value measured when the

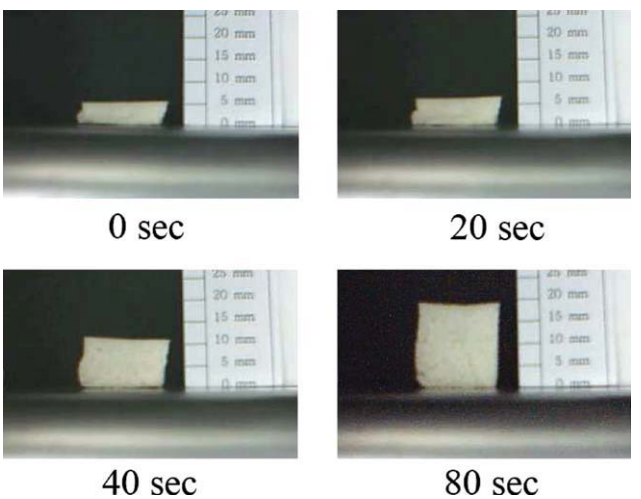

Figure 7 The shape recovery behavior for the foam measured at 50°C. [Color figure can be viewed in the online issue, which is available at www.interscience.wiley.com.]

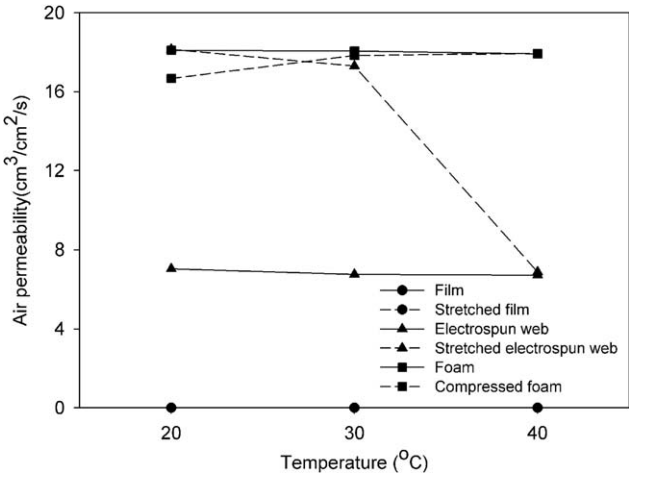

Figure 8 The air permeability of the specimens at different temperatures.

electrospun web was stretched in our previous research. When the foam was compressed by 80%, the foam density increased 5 times. Therefore, as the foam remained compressed at 20°C, the air permeability of the foam decreased slightly but showed no significant change compared with the original foam. When the foam recovered beyond the transition temperature, it showed an air permeability similar to the original foam. This is quite contrary to the permeability of the electrospun web having a porous structure. The air permeability of the stretched electrospun web increased 2.5 times at 20°C as compared with the original web. The electrospun web at 40°C, however, showed an air permeability similar to that of the original electrospun web, since it contracted almost to the original size above transition temperature because of the shape memory behavior. So, it means electrospun webs can change their pore size in accordance with the temperature change. It was observed that the foam generally had a higher

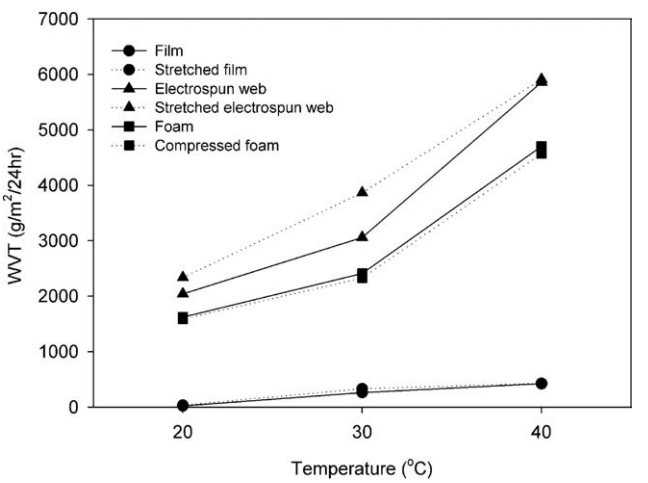

Figure 9 The water vapor transmission rate of the specimens at different temperatures.

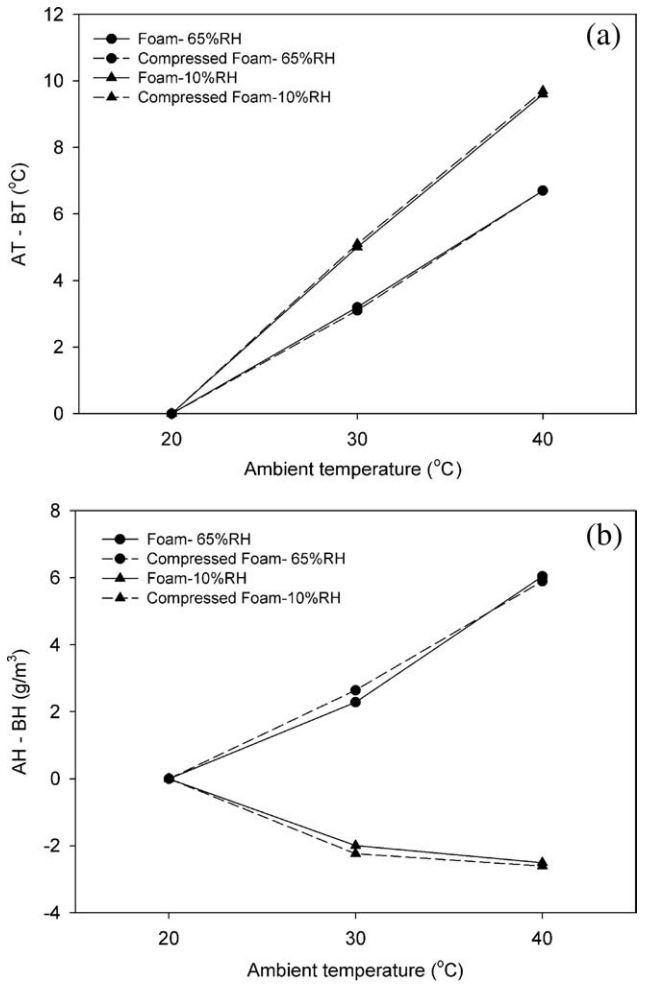

Figure 10 (a) The changes in interior temperature of a box covered by the foam at different ambient temperatures and relative humidities (thickness of foam: 20 mm, AT: Ambient temperature/BT: interior temperature of box). (b) The changes in the interior amount of water vapor of a box covered by foam at different ambient temperatures and relative humidities. (thickness of foam: 20 mm, AH: Ambient amount of water vapor/BH: interior amount of water vapor of box).

air permeability. This is probably attributable to the fact that foam, with a bigger cell size, is more favorable for air permeation.

Figure 9 shows the water vapor transmission rate (WVT) of the specimens. There was no significant difference in the WVT caused by a temperature increase between the compressed foam and the original foam. Moreover, as compared to the results of the previous research on the electrospun web, the cell size of the foam was much bigger than the pore size of the electrospun web, but the WVT of the foam was lower than that of the electrospun web. It can be inferred that since the thickness of the foam is greater than that of the electrospun web, it became a hindrance to water vapor permeation.

Thermal insulation property

Figure 10 shows the changes in temperature and amount of water vapor inside the insulating box covered by the foam after 1 h at various chamber temperatures and humidities. It was confirmed that there was a significant difference in the temperatures between the outside and inside of the insulating box, which was a proof that the foam had a high capability of thermal insulation. The compressed foam and the original foam showed a similar temperature differential between the outside and inside of the insulating box. In addition, the foam showed a bigger difference between the outside temperature and the inside temperature of the insulating box at a 65% RH than in a 10% RH. Specimens with the types of pores found in the foam have a lower capability of thermal insulation, possibly because water vapor can move to the inside of the specimen when the amount of water vapor increases with an external high heat.

The difference in the amount of water vapor between the outside and inside of the insulating box was slightly more significant for the foam that partially maintained its compressed shape at 30°C than for the original foam. This is probably due to the increase in the density of the compressed foam as compared with the original foam, which decreased the inside space where the water vapor could pass through. This led to a slightly lowered water vapor permeability.

Figure 11 shows the comprehensive comparison and evaluation of the test results in regard to the

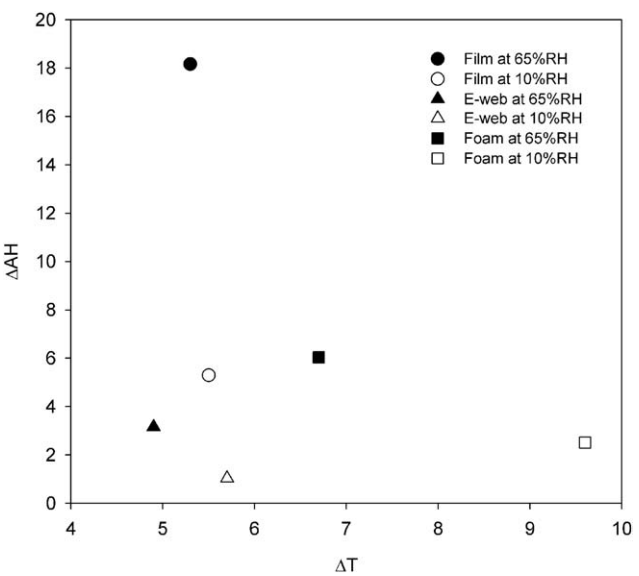

Figure 11 The thermal insulating properties and the water vapor permeabilities of the film, the electrospun web and the foam at an ambient temperature of 40°C (thickness of specimens: film: 40 μm, electrospun web: 40 μm, foam: 20 mm).

thermal insulation property of the film and the electrospun web used in our previous research and the foam. Generally, all the specimens showed a significant difference in the temperatures between the inside and outside of the insulating box in the dry environment of 10% RH, which means an improved thermal insulation capability. The film showed the biggest difference in the amount of water vapors between the inside and outside of the insulating box, which proved that the film had the lowest water vapor permeability. This property is expected to be a factor that impacts wearability, as it prevents sweat inside the clothes from evaporating. On the contrary, the electrospun web showed the smallest difference, which meant that the electrospun web had the highest water vapor permeability. Therefore, this property is expected to improve the wearability as it facilitates the evaporation of sweat inside the clothes. In addition, the foam showed the biggest temperature difference between the inside and outside of the insulating box, which proved that the foam had the highest thermal insulation capability along with a relatively high water vapor permeability. This property is expected to prevent sweat inside clothes from being discharged to some degree. However, the foam is expected to be used for protective clothing with the highest capability of thermal insulation since it showed an excellent thermal insulation effect.

A limitation of these results is that the film, the electrospun web, and the foam are different from one another in terms of thickness. But these comparisons and evaluations are still meaningful, as they are conducted in the consideration of membranes and fillers that can be used common. The results confirmed that the water vapor permeability and thermal insulation varied according to the type of material. Therefore, it is expected that the materials that show the maximum effect in a specific environment may be used depending on the properties of the various materials.

CONCLUSIONS

In this research, we manufactured the SMPU foam and examined the possibility of the foam being used as intelligent material whose capabilities were improved enough to insulate external heat under high temperature conditions. The transtion temperture of the SMPU foam was similar to that of film. The foam showed a very high capability of shape recovery and shape retention. It was observed that the permeabilities of the foam decreased slightly when the foam was compressed below the transition temperature, however the permeabilities of the foam did not vary noticeably after shape fixation because of its highly porous structure. In addition, the foam showed a very high capability of thermal insulation.

Therefore, it can be inferred that as the thickness of the foam is changed according to an ambient temperature the foam will remain thin with a fixed shape in a standard environment, which improves the wearability, and when the ambient temperature increases the foam will recover its thickness, with an improved thermal insulation capability.

References

1. Langenhove, V.; Hertleer, C. Int J Clothing Sci Technol 2004, 16, 63.
2. Mattila, H. Intelligent textile and clothing; Woolhead publishing Limited: Cambridge, 2006; p 95.
3. Schmidt, A. Macromol Rapid Commun 2006, 27, 1168.
4. Lendlein, A.; Jiang, H.; Junger, O.; Langer, R. Nature 2005, 434, 879.
5. Scott, T.; Schneider, A.; Cook, W.; Bowman, C. Science 2005, 308, 1615.
6. Liu, C.; Qin, H.; Mather, P. T. J Mater Chem 2007, 17, 1543.
7. Kim, B. S.; Lee, S. H.; Furukawa, F. Handbook of Condensation Thermoplastic Elastomers; Wiley-VCH: Weinheim, 2005; p 521.
8. Behl, M.; Lendlein, A. Mater Today 2007, 10, 20.
9. Ratna, D.; Karger-Kocsis, J. J Mater Sci 2008, 43, 254.
10. Fu, Y.; Du, H.; Huang, W.; Zhang, S.; Hu, M. Sens Actuators A 2004, 112, 395.
11. Meng, Q.; Hu, J.; Mondal, S. J Membr Sci 2008, 319, 102.
12. Ding, X.; Hu, J.; Tao, X. J Appl Polym Sci 2008, 107, 4061.
13. Chen, Y.; Liu, Y.; Fan, H. J Membr Sci 2007, 287, 192.
14. Mondal, S.; Hu, J. Des Monom Polym 2006, 9, 527.
15. Lee, S. H.; Jang, M. K.; Kim, S. H.; Kim, B. K. Smart Mater Struct 2007, 16, 2486.
16. Prima, M.; Lesniewski, M.; Gall, K.; Mcdowell, D.; Sanderson, T.; Campbell, D. Smart Mater Struct 2007, 16, 2330.
17. Tobushi, H.; Matsui, R.; Hayashi, S.; Shimada, D. Smart Mater Struct 2004, 13, 881.
18. Tobushi, H.; Okumura, K.; Endo, M.; Hayashi, S. J Intell Mater Syst Struct 2001, 12, 283.
19. Tey, S.; Huang, W.; Sokolowski, W. Smart Mater Struct 2001, 10, 321.
20. Metcalfe, A.; Desfaits, A.; Salazkin, I.; Yahia, L.; Sokolowski, W.; Raymond, J. Biomaterials 2003, 24, 491.
21. Small, W. IEEE Trans Biomed Eng 2007, 54, 1157.
22. Huang, W.; Lee, C.; Teo, H. J Intell Mater Syst Struct 2006, 17, 753.
23. Mikos, A.; Sarakinos, G.; Leite, S.; Vacanti, J.; Langer, R. Biomaterials 1993, 14, 323.
24. Nam, Y. S.; Yoon, J. J.; Park, T. G. J Biomed Mater Res 2000, 53, 1.